Journal of Control, Automation and Electrical Systems (2018) 29:670–676
https://doi.org/10.1007/s40313-018-0416-5

Experimental Characterization and Control of a Force Actuator Based on Shape Memory Alloy Wire

Samuel de Oliveira[1] · Simplício A. Silva[1] · Cícero R. Souto[1] · Andreas Ries[1]

Received: 15 March 2018 / Revised: 14 August 2018 / Accepted: 26 August 2018 / Published online: 3 September 2018

Abstract
This paper presents an experimental design of a force and position controller for a Ni–Ti shape memory alloy actuator. The focus of this work is a measurement device for the characterization of a SMA spring together with the fuzzy controller for position and force that can be quickly and easily implemented. This device makes it possible to develop a mechanism for robotic applications with slow actuation speed, e.g., to mimic a robotic finger. The contribution of our work to the scientific literature is an easy control of force and position, as well as weight reduction when compared to a similar actuator controlled by a traditional electric motor. Ni–Ti wire was winded up to form a coil; an electric current passing through the actuator changes its temperature, which leads to a phase transformation resulting in a length change of the wire. Thus, the actuator behaves as a spring, whose force exerted can be adjusted by an electric current. A closed-loop fuzzy logic controller was programmed in the LabVIEW environment, allowing the control of the force exerted by the actuator, as well as the position of an attached load. The actuator performance was evaluated experimentally before and after a training session.

Keywords Shape memory alloy · Nickel–titanium alloy · Fuzzy logic · Actuator

1 Introduction

Shape memory alloys (SMAs) are a well-known class of smart materials. When subjected to certain thermal cycling, mechanical work is generated through the recovery of a predetermined shape (Nespoli et al. 2010). In the field of robotics, these materials are known as "artificial muscles" due to their ability to generate movements similar to a human muscle. However, features such as the high force to weight ratio, the quiet and smooth movements, the absence of gear problems, mechanical failures and wear, make SMAs very attractive for numerous applications.

✉ Andreas Ries
ries750@yahoo.com.br

Samuel de Oliveira
eng.samuel@ymail.com

Simplício A. Silva
simplicioarnaud@gmail.com

Cícero R. Souto
cicerosouto@cear.ufpb.br

[1] Electrical Engineering Department, Federal University of Paraiba, Cidade Universitaria s/n, João Pessoa 58051-900, Brazil

Shape memory alloys (SMAs) are metals with the ability to "memorize" their original shape. The study of the history and development of SMAs provides insight regarding Ni–Ti, a material relevant for recent developments. Its various applications made it increasingly important and visible on the world market. Nickel–titanium alloys are currently the most commonly used SMAs, but other alloys, for instance copper–aluminum–nickel, copper–zinc–aluminum and iron–manganese–silicon have found important applications too (Borden 1991).

The generic name of the Ni–Ti SMA family is "nitinol", an acronym for "Nickel Titanium Naval Ordnance Laboratory". Ni–Ti was discovered in 1961 almost by accident by William J. Buehler, a researcher with the Naval Ammunition Laboratory in White Oak, Maryland. Buehler found that nitinol can change its phase in the solid state (Kauffman and Mayo 1993). Today those phase transformations are known as martensitic and austenitic; they involve a rearrangement of atomic positions within the crystalline structure of the solid body (Kauffman and Mayo 1993). The austenite phase is a relatively hard phase, preferred at high temperature, and possesses a symmetrical cubic structure. In this phase, the alloy presents a relatively high elastic modulus (Hesselbach 1999). The martensite phase is flexible, easily deformable

and possesses a structure with low symmetry (Hesselbach 1999).

Figure 1 shows schematically the evolution of the volumetric martensite fraction versus temperature, assuming the material is not subjected to a mechanical strain (Delaey et al. 1974). The SMAs present a thermomechanical behavior heavily dependent on temperature, exhibiting two distinguishable properties: superelasticity (SE) and shape memory effect (SME).

SME can be defined as the recovery process in a way that occurs by increasing the temperature of the alloy, in other words, the deformation undergone by the material is recovered when it is heated at temperatures higher than the A_f (Final Austenite Temperature).

SE is a property coupled to the SME. It is characterized by a phase transformation (and consequently the shape recovery) without the requirement of SMA temperature change (Otsuka and Wayman 1998).

Due to these characteristics, SMAs have found a wide range of applications, for instance in medical devices, security and robotics. However, there is a large hysteresis in their thermomechanical response during the phase transformation cycle. It is mainly caused by friction associated with the movement of the austenite-martensite interfaces and martensite-martensite interfaces with different crystallographic orientations (Bo and Lagoudas 1999).

Studies on SMA actuators have already been reported in the literature. According to Ahn and Kha (2008), nonlinear hysteresis effects existing in SMA actuators are a challenge for motion control; based on numerical simulations, these authors suggested that a combination of fuzzy logic and the numerical Preisach model provides reasonable control results. Later on, they developed successfully a feedforward and feedback control strategies (Nguyen and Ahn 2009) as well as a self-tuning fuzzy PID controller (Ahn and Kha 2006). According to Rohani et al. (2008), such self-tuning fuzzy controllers lead to a superior control performance.

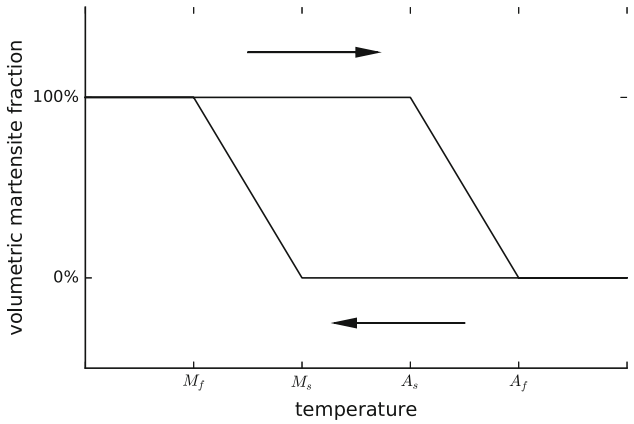

Fig. 1 Volumetric martensite fraction as a function of temperature

Applications based on SMA wires generate typical displacements between 5 and 7% (Silva et al. 2013). The main advantage of SMA spring coils is a reduced actuator volume; here the displacement can reach values over 300% of the initial length. However, the actuator force is a function of the elastic constant. Thus, the force behavior of the coil has to be characterized for controller implementation.

This work presents a fuzzy controller design for self-tuning the SMA spring, thus, controlling its position and force. The methodology was based on the literature, where many studies show characterizations of actuators of various types and geometries (Yang and Gu 2002; Zhong and Yeong 2006; Wang et al. 2008; Leester-Shädel et al. 2008; Lee and Kim 2008; Torres-Jara et al. 2010). The control system is based on fuzzy logic, with either the force or the displacement being the control variable. This means in case the force was being controlled, the displacement was observed and vice versa. We determined the actuator's behavior with and without training the force and displacement control.

Besides that, we investigated the possibility of an intelligent controller strategy, using the SMA spring without the need for training; so this work contributes to new control strategies in automation and robotic industry.

2 Materials and Methods

2.1 Actuator Construction

This work considers a SMA actuator in the form of a helical spring. The actuator was made from 983 mm Nickel–titanium (Ni–Ti) wire of (1.016) mm diameter, resulting in an average actuator diameter of 12 mm. Its initial length was 60 mm, and with the variation of temperature between 27 and 150 °C it allowed a displacement of 250%, that is, the spring recovered in the form of a variation from 150 to 60 mm. Figure 2 shows a photograph of the spring-shaped actuator, mounted on a metal rod with hose clamps.

Prior to any experiments, the SMA actuator was heat treated at 450 °C for 25 min in order to release a possible internal stress of the material and to imprint the desired shape. Afterward, the actuator cooled down to room temperature in ambient air.

Fig. 2 Fabrication of the SMA actuator

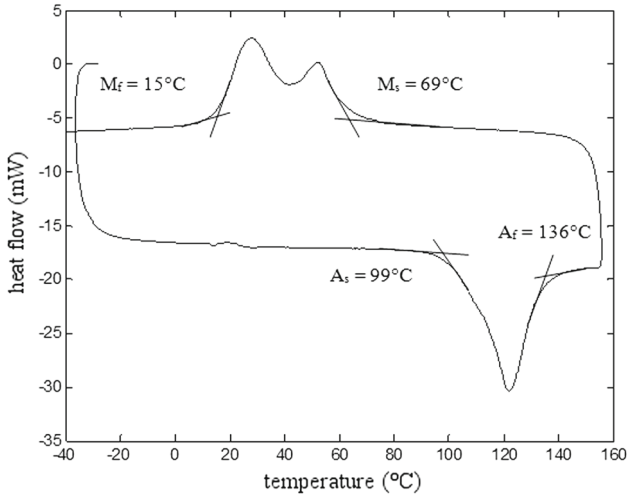

Fig. 3 Differential scanning calorimetry measurement of a Ni–Ti wire after heat treatment at 450 °C for 25 min

After the heat treatment, a small piece of wire was cut for a differential scanning calorimetry test, in order to determine the temperature ranges of the phase transformations. As shown in Fig. 3, the martensite phase forms upon cooling from 69 to 15 °C, while the austenite phase forms in the approximate temperature range from 99 to 136 °C.

2.2 Experimental Setup for Measuring Actuator Performance

For applications of the SMA actuator, as well as for the characterization of the displacement and force control, a special mechanical device was constructed, transforming length changes of the actuator spring into a horizontal movement.

This device comprises a fixed base and two movable ends fastened to two metal rods that slide almost frictionless through the fixed base. Both ends of the metal rods were fixed to plastic terminals, thus were held at a constant distance in order to prevent any misalignment when the actuator operates. Connectors have been developed to mount the spring to the base and one terminal. Figure 4 shows schematically the mechanical configuration, highlighting each element.

The experiment outlined in Fig. 4 is related to the characterization of the SMA spring under dynamic condition, where attention is given to the displacement of the device. Under static condition, the force that the SMA spring can apply to the structure is recorded. The final experiment according to Fig. 5 deals with full actuator application (SMA springs). The difference between this experiment and the actuation of a robotic finger (see Silva et al. 2013) is the constant weight to be lifted.

A SMA spring (actuator) was attached to the connectors between the base and a terminal. A common spring (stiffness k = 595.35 N/m) in series with a load cell connects the base

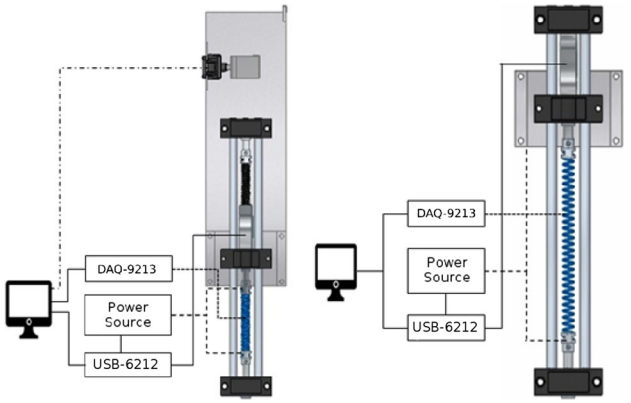

Fig. 4 Schematic diagram of the force position controller circuitry. Left: Dynamic characterization. Right: Static characterization

and the second terminal, measuring the force (see Fig. 4, left part).

This structure allows three different evaluations: (1) the dynamic characteristics of the actuator on the structure; monitoring the movement of one of the terminals, thus allowing a control of its shifting, as shown in Fig. 4 left part; (2) the static characteristics, determining the maximum force and intermediate variations of the force that the actuator is able to impose on the structure, as shown in Fig. 4, right part; and (3) the last configuration for training the actuator, see Fig. 5.

For the dynamic actuator characterization, a video camera, installed at 150 mm height above the base, served as a displacement sensor. Its focus was adjusted to a terminal, between the outer edge and the clamping screw (see Fig. 4 left part). The camera settings were set for capturing 640x480 pixel grayscale images and 75 photos per second, leading to a 0.001 mm displacement resolution.

For static characterizations, a load cell is directly mounted between a terminal and the base (Fig. 4 right part). In this case, the actuator imposes a pulling force on the terminal, which is then transferred to the second terminal through the base, (slidable, located between two aluminum guides); this allows a measurement of the force via load cell.

In the setup for training the actuator, a distance holder (35 mm PVC plastic) was fixed to the free terminal (1 in Fig. 5), limiting the maximum elongation of the SMA spring connected to the second terminal in series with a load cell attached to the base (2 in Fig. 5). A mass of 1.2 kg (5 in Fig. 5)was attached to the actuator by means of a steel wire (4 in Fig. 5) suspended using a metal rod (3 in Fig. 5) at the lateral of the setup. The admitted load (1.2 kg) was based on the literature convention, choosing 80% of the maximum load that the actuator could move experimentally (Farias et al. 2012).

The untrained actuator was manufactured as described previously. This means after winding, the SMA was heat treated at 450 °C for 25 min and characterized after cooling

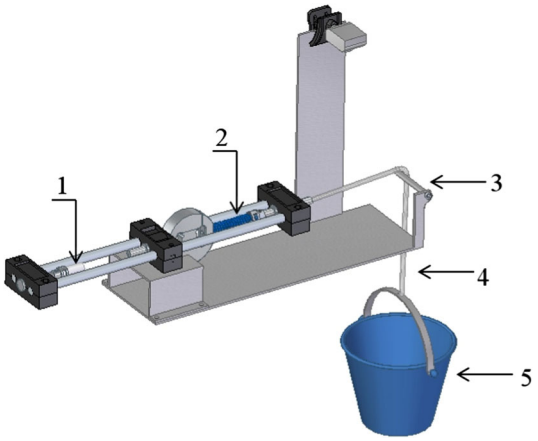

Fig. 5 Experimental setup used for actuator training. (1) PVC distance holder. (2) Shape memory alloy actuator. (3) Metal rod. (4) Stainless steel wire. (5) Mass support

down to room temperature. The trained actuator, was equally manufactured and then additionally subjected to a controlled training process. The training consisted of 1000 complete cycles of mechanical deformation and heating to recover the initial state. Each complete cycle corresponded to 150% traction deformation at room temperature (deformed state, was held for 35 s), followed by heating to 150 °C for 25 s to achieve shape recovery (recovered state). A controller regulated the electrical current through the actuator in order to achieve this temperature.

The actuator was characterized by force control tests and displacement control tests, both with and without the training session. Mass displacements were observed as actuator reactions due to predefined force variations. In a similar way, forces were measured upon mass displacements.

By means of the two experimental configurations shown in Fig. 4, four different experiments lead to data collection: (1) Untrained actuator controlling the force; displacement observed. (2) Untrained actuator controlling the displacement; force measured. (3) Trained actuator controlling the force; displacement observed. (4) Trained actuator controlling the displacement; force measured.

Force control was achieved using the static setup (Fig. 4, right part); for displacement control, the dynamic set up (Fig. 4, left part) has to be used. Data were collected via the NI-USB-6212 interface (force and displacement), as well as the DAQ-9213 interface, which was connected to a K-type thermocouple recording the temperature of the SMA actuator. The thermocouple was connected to the center of the SMA spring by resistance spot welding. Both ends of the SMA spring were fixed by means of stainless steel clamping connectors, which were in electrical contact with the power supplying wires. The mounting structure consisted of non-conductive polymeric material, thus, there was no need to develop an electrical isolation module.

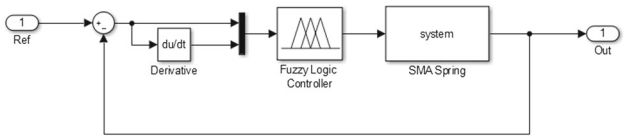

Fig. 6 Fuzzy controller wiring diagram

The training routine and the fuzzy controller were programed in the LabView environment. A Mamdani-type fuzzy controller was implemented. The control variable definitions were created due to error and error variation, with a universe of discourse normalized between -1 and 1. For the output variable, the universe of discourse was discrete between 0 and 6, this being the voltage used to control the current amplification module. Figure 6 shows the scheme used to implement the fuzzy controller.

3 Results and Discussion

Two different characterizations are interesting. First, the peak force of the SMA actuator was measured together with its time dependent temperature (static test, Fig. 4). Then the dynamic test records the maximum mass displacement achieved by the actuator, again together with the temperature profile of the actuator (Fig. 4).

As shown in Fig. 7, utilizing the static configuration makes it possible to determine the force; the actuator is able to produce a peak force of 7.5 N. The dynamic configuration allows the determination of the displacement. Here the maximum displacement value is 18 mm, while the actuator temperature rises up to 160 °C.

From these data, it was possible to program a Mamdani-type fuzzy controller, where the definition of control variables is related to the error and the error variation. With the fuzzy set normalized, two trapezoidal and five triangular membership functions were chosen for both, the input and output variables. Each variable has seven linguistic qualifiers, called: NB (negative big), NM (negative medium), NS (negative small), ZE (zero), PS (positive small), PM (positive medium), PB (positive big). The center of area method was applied for defuzzification; control rules were established as shown in Table 1.

The fuzzy rules are given by the following representations:

$$\text{Error} = \{(x, \mu_1(x))|\ x \in (0, 1)\} \quad (1)$$

$$\text{Err}_{\text{var}} = \{(x, \mu_2(x))|\ x \in (0, 1)\} \quad (2)$$

The inference method used was the Mamdani Method. It combines the degrees of membership referring to each of the input values, given by Center of Area (CoA).

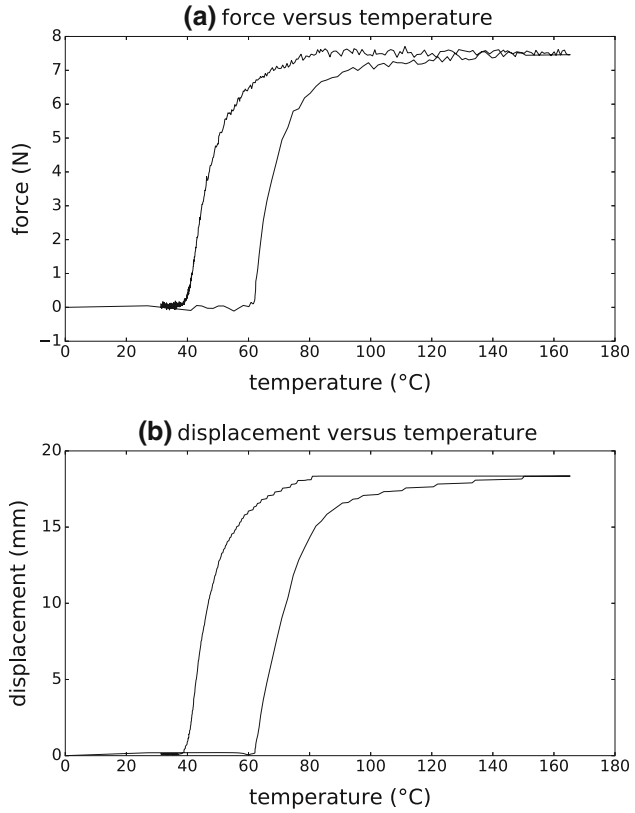

Fig. 7 Actuator response to a voltage pulse: **a** static configuration, **b** dynamic configuration

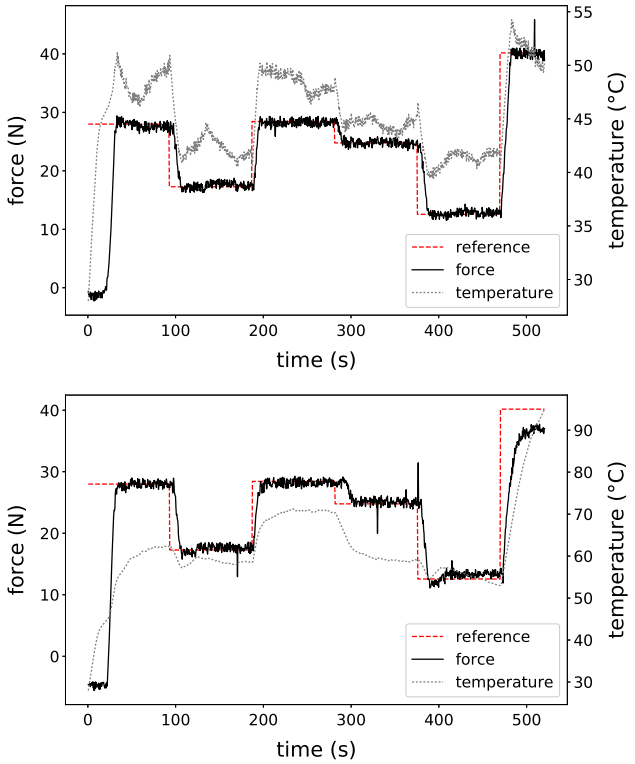

Fig. 8 Force control using the dynamic configuration: without training (top), with training (bottom)

Table 1 Fuzzy if-then rules

Error/Err. Var.	NB	NM	NS	ZE	PS	PM	PB
NB	NB	NB	NB	NB	NB	NS	ZE
NM	NB	NB	NB	NB	NM	ZE	PS
NS	NB	NB	NB	NB	ZE	PS	PM
ZE	NB	ZE	NM	NM	NS	PM	PB
PS	NM	NS	PM	PB	PB	PB	PB
PM	NS	ZE	PS	PM	PB	PB	PB
PB	ZE	PS	PM	PB	PB	PB	PB

$$\mathrm{CoA} = \frac{\int x\mu(x)\,\mathrm{d}x}{\int \mu(x)\,\mathrm{d}x} \tag{3}$$

According to Fig. 7 (also in agreement with the training), it can be concluded that the system is still time-varying, besides showing a large hysteresis. This behavior makes it difficult to implement a PID controller for this type of material. This actuator requires the use of more robust controllers that can "understand" the phase transformations inherent to the material and adapt properly. For a given reference current or reference voltage, there are two associated displacement or force values, which depend on the direction of the phase transformation. This is the reason for choosing a fuzzy logic controller, which has the advantage of an easy implementation, little data processing and computational time. Other controllers such as neural or adaptive types are high performers, but often require more complicated learning rules, more data processing and computational time.

Figure 8 shows the force control results, only the mass shift by the actuator was monitored, distinguishing the trained and untrained controller. Figure 9 shows the observed displacement when the control force was applied to the actuator.

Figures 10 and 11 show the position control results; again the actuator force was recorded for the trained and untrained actuator. Without training, the actuator performed with higher positioning accuracy, due to the significant temperature difference between the two control regimes. In case of the untrained actuator, the positioning error varied around 2.5%, while after the training, the error became 8.8% and the mean operating temperature was increased by 14 °C, considering the same reference displacements.

From Fig. 10, it is possible to verify the displacement (dynamic configuration), using the SMA spring with and without training. It can be seen that after 250 s, the response of the untrained actuator is faster than that of the trained one. The objective of the training was to prevent that the actuator first generates a force or a displacement above/below the reference value and then reaches the desired reference

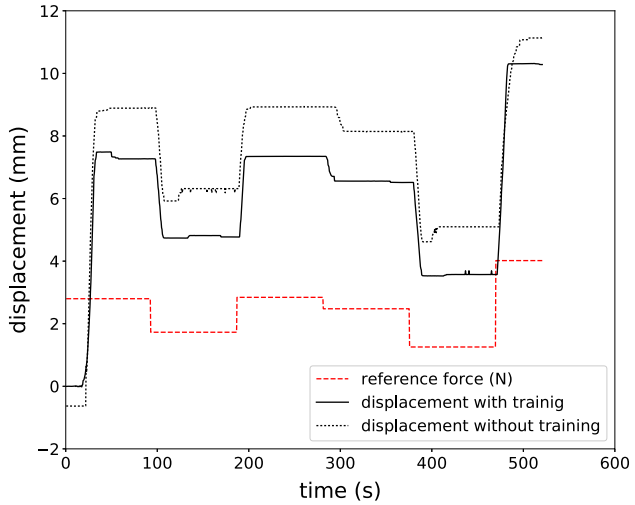

Fig. 9 Observed displacement with and without training

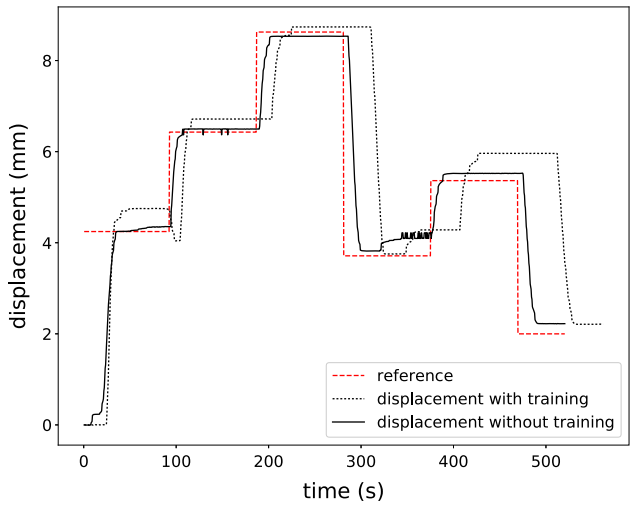

Fig. 10 Position control in dynamic configuration. Actuator with and without training

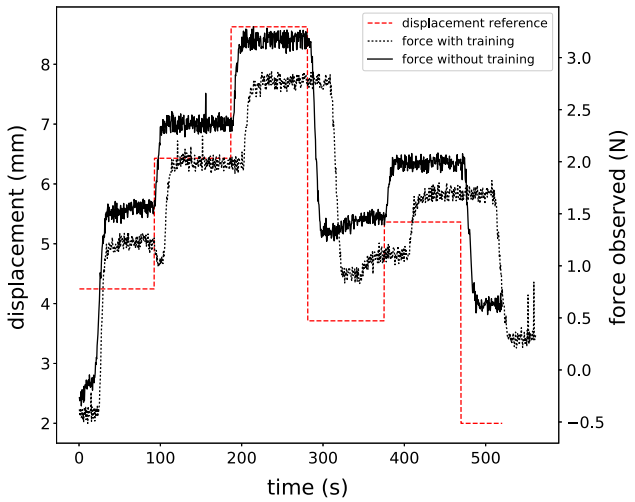

Fig. 11 Force control in dynamic configuration. Actuator with and without training

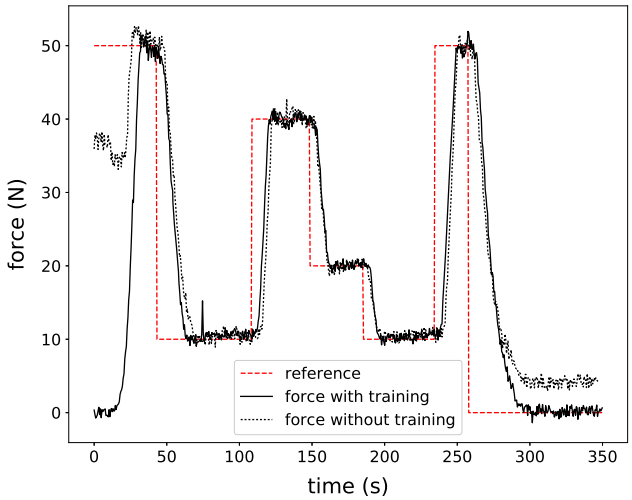

Fig. 12 Force control, static structure

value (overreaction). In that way, it can be understood that the actuator training did not optimize the response time.

Figure 12 displays the displacement variation and the force observed to produce this displacement considering different actuation times for the trained and untrained case. The untrained actuator had an initial force, and it is expected that 300 s of actuation time are not sufficient to eliminate the existing residual force, as can be seen in Fig. 11. As expected, the untrained actuator exhibits a residual force; after some control cycles, a value close to 5 N was reached. The trained actuator did not present a significant residual force, neither at the beginning, nor at the end of the experiment. The intermediate reference forces were reached by the actuator with no significant difference between the trained and untrained case.

The results are comparable with those by Silva et al. (2013); these authors used SMA wires for the movement of fingers; our work provides the advantage of a much smaller actuator due to the spring form. Regarding the displacement and force control, our fuzzy controller showed a performance equivalent to that of a genetic algorithm used by Ahn and Kha (2008). Thus, our SMA spring can be used as a tendon for movement of fingers and feet in the field of robotics and prosthesis.

Tai et al. (2010) performed a position and force control using a GPC (Generalized Predictive Control) also considering a SMA spring. These authors obtained results similar to those obtained by our controller. The advantage of our setup is the simplicity of controller implementation.

4 Conclusions

The results demonstrate the ability to use the SMA spring actuator as a unidirectional actuator in both cases, with or without training. Without training, the actuator achieves the same force as when trained, however with the advantage of an approximately 14 °C lower operation temperature. The disadvantage of the untrained actuator is a lack of final stabilization. The trained actuator oscillated significantly less over the reference point; however, its working temperature was higher. For accurate position control, the untrained SMA actuator has the advantage of exerting less force to achieve the reference when compared to the trained actuator.

Acknowledgements The authors would like to thank CAPES for financial support.

References

Ahn, K. K., & Kha, N. B. (2006). Position control of shape memory alloy actuators using self tuning fuzzy PID controller. *International Journal of Control, Automation, and Systems*, *4*, 756–762.

Ahn, K. K., & Kha, N. B. (2008). Modeling and control of shape memory alloy actuators using Preisach model, genetic algorithm and fuzzy logic. *Mechatronics*, *18*(3), 141–152. https://doi.org/10.1016/j.mechatronics.2007.10.008.

Bo, Z., & Lagoudas, D. C. (1999). Thermomechanical modeling of polycrystalline SMAs under cyclic loading, Part IV: Modeling of minor hysteresis loops. *International Journal of Engineering Science*, *37*(9), 1205–1249.

Borden, T. (1991). Shape memory alloys: Forming a tight fit. *Mechanical Engineering*, *113*(10), 67–72.

Delaey, R., Krishnan, H., & Warlimont, H. (1974). Thermoelasticity, pseudoelasticity and the memory effects associated with martensitic transformations Part 1: Structural and microstructural changes associated with the transformations. *Journal of Materials Science*, *9*, 1521–1535.

Farias, J. d. S., Alves, D. N. L., Souto, C. d. R., da Silva, S. A., & de Araújo, C. J. (2012). Comportamento do treinamento de fios atuadores com memória de forma submtidos a diferentes amplitudes de ondas de corrente elétrica. CONEM2012, pp. 1–8.

Hesselbach, J. (1999). Shape memory actuators. In H. Janocha (Ed.), *Adaptronics and smart structures* (pp. 143–160). Berlin: Springer.

Kauffman, G., & Mayo, I. (1993). Memory metal. *Chem Matters*, 4–10.

Lee, S. K., & Kim, B. (2008). Design parametric study based fabrication and evaluation of in-pipe moving mechanism using shape memory alloy actuators. *Journal of Mechanical Science and Technology*, *22*, 96–102.

Leester-Shädel, M., Hoxhold, B., Lesche, C., Demming, S., & Büttgenbach, S. (2008). Micro actuator on the basis of thin SMA foils. *Microsystem Technologies*, *14*, 697–704.

Nespoli, A., Besseghini, S., Pittaccio, S., Villa, E., & Viscuso, S. (2010). The high potential of shape memory alloys in developing miniature mechanical devices: A review on shape memory alloy mini-actuators. *Sensors and Actuators A: Physical*, *158*(1), 149–160. https://doi.org/10.1016/j.sna.2009.12.020.

Nguyen, B. K. N. B. K., & Ahn, K. A. K. (2009). Feedforward control of shape memory alloy actuators using fuzzy-based inverse Preisach model. *IEEE Transactions on Control Systems Technology*, *17*(2), 434–441. https://doi.org/10.1109/TCST.2008.924580.

Otsuka, K., & Wayman, C. M. (1998). *Shape memory materials* (p. 284). Cambridge: Cambridge University Press.

Rohani, O., Yousefi-Koma, A., Rezaeeian, A., & Doosthoseini, A. (2008). Force control of shape memory alloy wire using fuzzy controller. In: *Proc. SPIE 6926, Modeling, Signal Processing, and Control for Smart Structures* (Vol. 6926, Art No. 692611). https://doi.org/10.1117/12.776405.

Silva, A. F. C., dos Santos, A. V., da Rocha Souto, C., de Araújo, C. J., & da Silva, S. A. (2013). Artificial biometric finger driven by shape-memory alloy wires. *Artificial Organs*, *37*(11), 965–972. https://doi.org/10.1111/aor.12227.

Tai, N. T., Kha, N. B., & Ahn, K. K. (2010). Predictive position and force control for shape memory alloy cylinders. *Journal of Mechanical Science and Technology*, *24*(8), 1717–1728. https://doi.org/10.1007/s12206-010-0504-3.

Torres-Jara, E., Gilpin, K., Karges, J., Wood, R. J., & Rus, D. (2010). Composable flexible small actuators built from thin shape memory alloy sheets. *Robotics & Automation Magazine*, *17*, 78–87.

Wang, Z., Hang, G., Li, J., Wang, Y., & Xiao, K. (2008). A Micro-robot fish with embedded SMA wire actuated flexible biomimetic fin. *Sensors and Actuators A: Physical*, *144*, 354–360.

Yang, K., & Gu, C. L. (2002). A Novel robot hand with embedded shape memory alloy actuators. *Journal of Mechanical Engineering Science*, *216*, 737–745.

Zhong, Z. W., & Yeong, C. K. (2006). Development of a gripper using SMA wire. *Sensors and Actuators A: Physical*, *126*(2), 375–381. https://doi.org/10.1016/j.sna.2005.10.017.